Hindawi
Journal of Combustion
Volume 2017, Article ID 6160234, 7 pages
https://doi.org/10.1155/2017/6160234

Research Article

Decomposition Characteristics and Kinetics of Microalgae in N_2 and CO_2 Atmospheres by a Thermogravimetry

Xu Qing,[1,2] Ma Xiaoqian,[1] Yu Zhaosheng,[1] Cai Zilin,[1] and Ling Changming[2]

[1]*School of Electric Power, South China University of Technology, Wushan Road 381, Tianhe District, Guangzhou City 510640, China*
[2]*School of Mechanical and Power Engineering, Guangdong Ocean University, Jiefang Road 40, Xiashan District, Zhanjiang City 524025, China*

Correspondence should be addressed to Ma Xiaoqian; epxqma@scut.edu.cn

Received 20 September 2016; Revised 28 November 2016; Accepted 14 February 2017; Published 15 March 2017

Academic Editor: Kazunori Kuwana

The thermal degradation characteristics of microalgae were investigated in highly purified N_2 and CO_2 atmospheres by a thermogravimetric analysis (TGA) under different heating rates (10, 20, and 40°C/min). The results indicated that the total residual mass in CO_2 atmosphere (16.86%) was less than in N_2 atmosphere (23.12%); in addition, the kinetics of microalgae in N_2 and CO_2 atmospheres could be described by the pseudo bicomponent separated state model (PBSM) and pseudo-multi-component overall model (PMOM), respectively. The kinetic parameters calculated by Coats-Redfern method showed that, in CO_2 atmosphere, the apparent activation energy (E) of microalgae was between 9.863 and 309.381 kJ mol^{-1} and the reaction order (n) was varied from 1.1 to 7. The kinetic parameters (E, n) of the second stage in CO_2 atmosphere were quite similar to those in N_2 atmosphere.

1. Introduction

Renewable and clean energy has become more and more important globally, especially with the current fuel crisis, economic crisis, and environmental pollution [1]. The bioenergy, as one form of renewable energy, is widely used in the third world. Its application can not only relax the energy crises but also restrain the environmental pollution [2, 3]. However, in recent years, the competition over biomass supply for fuel or for food has been intensified, which has resulted in growing interests in alternative, nonedible biomass resources such as perennial rhizomatous grasses, miscanthus (*Miscanthus*), and switch grass (*Panicum virgatum*) [4].

Microalgae have many advantages over existing energy crops, such as faster growth rate, shorter growth time, higher biomass production, biochemicals and higher volume carbon abatement and no demand on arable land [5–8]. Furthermore, there is a possibility of direct generation of desired end products like bio-oil and hydrogen to be processed afterwards (like starch and biomass) [9]. Microalgae, as a source of biofuels and technological solution for CO_2 fixation, are subject to intense academic and industrial research in its potential [10].

Pyrolysis is the degradation of macromolecular materials with heat alone in absence of oxygen [11]. In recent years, many researches have studied the pyrolysis characteristics of microalgae in N_2 atmosphere and established significant information on the pyrolysis behavior and kinetics [7, 11–13]. Both N_2 and CO_2 are inert gases. However, there have been no reports on the decomposition characteristics of microalgae in CO_2 atmosphere. Whether the decomposition characteristics of microalgae in CO_2 atmosphere are the same as in N_2 atmosphere is still unknown.

Chlorella, a genus of unicellular green microalgae, with a spherical shape of 2.0~10.0 μm in diameter, living in both fresh and marine water, can generally be found in fresh water of ponds and ditches, moist soil, or other damp conditions, for example, the surface of tree trunks, water pots, and damp walls [14]. *Chlorella* includes eight species, one of which is *Chlorella vulgaris (C. vulgaris)*, growing in fresh water. Some scholars studied the pyrolysis kinetic of microalgae in N_2 atmosphere by TGA [15, 16]. Besides, the

conventional combustion, oxy-fuel combustion and hybrid combustion characteristics on microalgae were studied under different conditions by TGA [17–20]. However, the pyrolysis characteristics and kinetic analysis of microalgae pyrolysis under N_2 and CO_2 atmosphere by TGA were not reported yet.

So far the pyrolysis technology is still in development. The less reports on the pyrolysis of *C. vulgaris* in different atmospheres (N_2 and CO_2) were found. In this study, the decomposition characteristics of *C. vulgaris* were studied by a thermogravimetric analysis (TGA), and the effects of atmospheres (N_2 or CO_2 atmosphere) and heating rates (10, 20 and 40°C/min) on *C. vulgaris* decomposition were investigated. Finally, kinetic triplets of *C. vulgaris* were obtained with Coats-Redfern approximation method, including E, reaction order (n), and preexponential factor (A). Thermogravimetric date (TG) and differential thermogravimetry (DTG) profiles, pyrolysis characteristics, the effects of heating rate, and kinetics analysis were analyzed to determine the optimal conditions for *C. vulgaris* treatment process.

2. Material and Method

2.1. Sample Preparation. The powder of microalgae, *C. vulgaris,* was used in this study provided by Jiangmen YueJian Biotechnologies Co, Ltd. (Guangdong Province, China). The ultimate analysis and proximate analysis were tested according to GB/T212-2008 [21], GB211-84 [22], and ASTM D5373-08 [23], respectively. Heat values were done based on ASTM D5468-02 [24] and ASTM E870-82 [25]. The proximate analysis, ultimate analysis, and low calorific value were listed in Table 1. The *C. vulgaris* sample was dried in an oven at 105°C for 20 h and then milled and sieved with a screen of less than 200 μm in diameter. After the above treatment, the sample was stored in a desiccator for test.

2.2. Decomposition Experiment. Decomposition was carried out on NETZSCH STA 409 PC simultaneous analyzer with the heating rate of 10, 20, and 40°C/min from room temperature to 1000°C in either N_2 or CO_2 atmosphere. About 6 ± 0.2 mg dried sample was used for each run in nonisothermal conditions. The thermogravimetric (TG) and differential thermogravimetric (DTG) data were used to differentiate the decomposition as well as estimate the kinetic parameters. Three repeated experiments were accomplished for data confirmation, in order to verify reproducibility and decrease the experiments error.

2.3. Characteristic Parameters of Temperatures. The initial and final thermal degradation temperatures represent how hard the reaction is. T_I is the initial degradation temperature which is defined as the intersection of the tangent and the horizontal curve, and the temperature at which the DTG has its peak value is the location of the TG curve tangent. T_F is the final degradation temperature which is obtained when the mass lose accounts for 98% of the total quality loss. DTG_{peak} is differential thermal gravity value at a peak temperature and T_{peak} is degradation peak temperature which is defined as the temperature at which the mass loss rate in DTG curve reached the local maximum. D_V is the average weight loss rate of the temperature ranged from 100 to 1000°C.

2.4. Kinetic Modeling. The kinetic equation of common type can be generally expressed as follows [26]:

$$\frac{d\alpha}{dt} = k(T)\, f(\alpha), \tag{1}$$

where α is the conversion degree, t (min) is time, T (K) is the absolute temperature, $f(\alpha)$ is a function, the type of which depends on the reaction mechanism, and $k(T)$ is the temperature dependent rate constant. $k(T)$ is usually described with the Arrhenius equation:

$$k = A \exp\left(-\frac{E}{RT}\right), \tag{2}$$

where A (min^{-1}) is preexponential or frequency factor, E ($kJ\,mol^{-1}$) is the activation energy, and R (kJ/mol·K) is the universal gas constant.

The function $f(\alpha)$ is expressed as follows:

$$f(\alpha) = (1-\alpha)^n, \tag{3}$$

where n is the reaction order.

The degree of conversion of the reduction process is expressed as follows:

$$\alpha = \frac{m_i - m_t}{m_i - m_\infty}, \tag{4}$$

where m_i is the initial mass of the sample, m_t is the mass of the sample at time t, and m_∞ is the final mass of sample in the reaction [27, 28].

By derivation of (2) and (3) in (1) and is integrated by using Coats-Redfern approximation method [29, 30], it becomes

$$\ln\left[\frac{g(\alpha)}{T^2}\right] = \ln\left[\frac{AR}{\beta E}\left(1-\frac{2RT}{E}\right)\right] - \frac{E}{RT}, \tag{5}$$

where

$$g(\alpha) = \begin{cases} -\ln(1-\alpha), & n = 1, \\ \dfrac{1-(1-\alpha)^{1-n}}{1-n}, & n \neq 1. \end{cases} \tag{6}$$

In general, β is the heating rate; the term of $2RT/E$ can be neglected since it is much less than 1. A plot of $\ln[g(\alpha)/T^2]$ against $1/T$ should result in a straight line of slope $-E/R$ for the correct reaction mechanism, as using the method to find the suitable model function $g(\alpha)$ (or $f(\alpha)$) of global decomposition kinetics. Once the form of $g(\alpha)$ is obtained, the apparent activation energy E and the frequency factor A can be calculated from the straight line in light of (5).

Table 1: Ultimate and proximate analysis and lower heating values of *Chlorella vulgaris* (on dry basis).

Ultimate analysis (wt%)					Proximate analysis (wt%)			$Q_{net,d}$ (MJ kg^{-1})
C	H	O	N	S	Volatile	Ash	Fixed carbon	
47.84	6.41	25	9.01	1.46	55.37	10.28	34.35	21.88

Note: $Q_{net,d}$, lower heating value on dry basis.

With the PMOM, the *C. vulgaris* is considered as three pseudo components and individually decomposed over a temperature range, which can be expressed as follows:

$$\frac{d\alpha}{dt} = \begin{cases} \dfrac{w_{10} - w_{1\infty}}{w_{10} - w_{3\infty}} \dfrac{d\alpha_1}{dT}, & w_{10} < w < w_{1\infty}, \\ \dfrac{w_{20} - w_{2\infty}}{w_{10} - w_{3\infty}} \dfrac{d\alpha_2}{dT}, & w_{1\infty} = w_{20} < w < w_{2\infty}, \\ \dfrac{w_{30} - w_{3\infty}}{w_{10} - w_{3\infty}} \dfrac{d\alpha_2}{dT}, & w_{2\infty} = w_{30} < w < w_{3\infty}, \end{cases}$$

$$\frac{d\alpha_1}{dT} = \frac{A_1}{\beta} \exp\left(-\frac{E_1}{RT}\right) f_1(\alpha_1), \quad w_{10} < w < w_{1\infty}, \tag{7}$$

$$\frac{d\alpha_2}{dT} = \frac{A_2}{\beta} \exp\left(-\frac{E_2}{RT}\right) f_2(\alpha_2), \quad w_{20} < w < w_{2\infty},$$

$$\frac{d\alpha_2}{dT} = \frac{A_3}{\beta} \exp\left(-\frac{E_3}{RT}\right) f_3(\alpha_3), \quad w_{30} < w < w_{3\infty},$$

where w is the mass percentage of solid and the subscripts 0 and ∞ refer to the initial and residual amounts, respectively. The subscripts 1, 2, and 3, respectively, correspond to the pseudo components 1, 2, and 3 [31–33].

The analogy to (7) is considered when single and three pseudo components are involved. To obtain the kinetic parameters, the TG-DTG information and a nonlinear regression scheme are used in fitting equations (5) and (6).

3. Results and Discussion

3.1. Decomposition Process. The thermogravimetry (TG) and differential thermogravimetry (DTG) curves of *C. vulgaris* decomposition at a heating rate of 10°C min^{-1} in two atmospheres are shown in Figures 1 and 2, respectively. From Figure 2, two noteworthy peaks in pyrolysis are shown in curves; the decomposition process in N_2 atmosphere can be divided into three stages for interpretation. The first stage is from room temperature to 140°C, corresponding to a loss of moisture and a slight volatile compound. The second one is from 140 to 550°C, where most of the organic materials are decomposed; this is the main decomposition process. The third one is from 550 to 1000°C; during this stage, the carbonaceous matters in the solid residuals are continuously decomposed at a very low rate.

As mentioned in the previous paragraph, in N_2 atmosphere, only one main decomposition stage occurs at the temperature range of 140–550°C, which is close to *Chlorella protothecoides* (150–540°C) reported by Peng et al. [11].

In CO_2 atmosphere, four stages could be distinguished during thermal degradation process of *C. vulgaris*. The first stage is from room temperature to 140°C (dehydration).

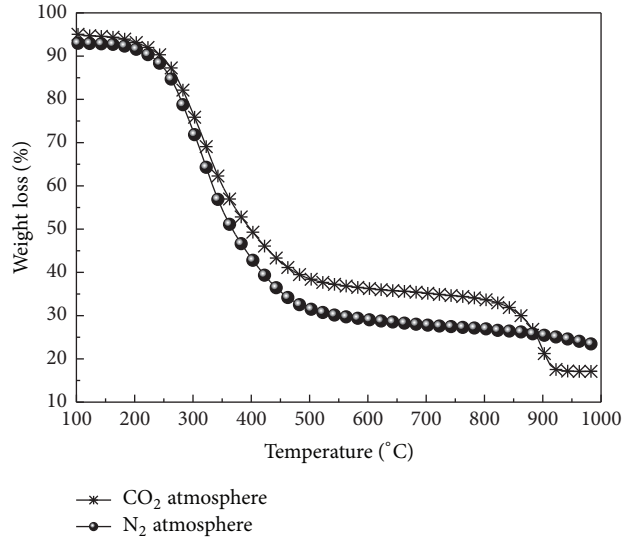

Figure 1: TG curves of *Chlorella vulgaris* decomposition at a heating rate of 10°C min^{-1} in N_2 and CO_2 atmospheres.

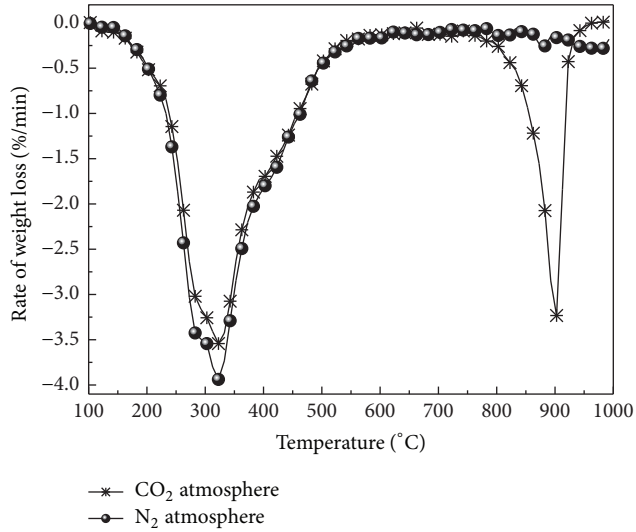

Figure 2: DTG curves of *Chlorella vulgaris* decomposition at a heating rate of 10°C min^{-1} in N_2 and CO_2 atmosphere.

The second one is from 140 to 560°C (devolatilization), corresponding to the first main decomposition process. The third one is from 560 to 790°C (devolatilization); at this stage, the rate of reaction is very low. The fourth one (second main decomposition process) is from 790 to 1000°C; in this stage, the residual carbonaceous matters and CO_2 may react at a relatively high rate. In CO_2 atmosphere, there are two

main decomposition stages (the second and fourth ones). Compared with the second stage, the fourth one is very narrow.

3.2. Comparison and Analysis of C. vulgaris Decomposition in N_2 and CO_2 Atmospheres. Figures 1 and 2 show that the TG and DTG curves of *C. vulgaris* decomposition in N_2 atmosphere are different from CO_2 atmosphere. As mentioned in Section 3.1, the decomposition process of *C. vulgaris* in N_2 atmosphere can be divided into three stages, and one main decomposition process is obtained. However, in CO_2 atmosphere, the thermal decomposition process is divided into four stages and two main decomposition processes are obtained.

In addition, as shown in Figure 1, when the temperature is below 887°C, the weight loss in CO_2 atmosphere is less than in N_2 atmosphere. The decomposition process of *C. vulgaris* in CO_2 atmosphere is delayed due to the difference of the CO_2 from N_2 molecule. When the temperature reaches 887°C, the weight loss of *C. vulgaris* decomposition in N_2 atmosphere is equivalent in CO_2 atmosphere. However, when the temperature is above 887°C, a quick increase in the weight loss is observed in CO_2 atmosphere, which may be caused by the gasification of carbonaceous matters.

The characteristic parameters for *C. vulgaris* decomposition can be obtained from Figure 2, as shown in Table 2. It is clear that there is a peak for the thermal decomposition process of *C. vulgaris* in N_2 atmosphere at 322°C, and at this temperature the rate of weight loss attains the maximum value. However, in CO_2 atmosphere, there are two peaks of the DTG curve occurring at 323.8°C and 901.1°C, respectively. The maximum rate of weight loss is attained at 323.8°C. The total residual mass in N_2 atmosphere is 23.12%, more than in CO_2 atmosphere (16.86%).

Figure 2 shows that in the low temperature range (210–470°C), the mass loss rate of *C. vulgaris* decomposition in CO_2 atmosphere is lower than in N_2 atmosphere, but between 760°C and 926°C, it is opposite. It may be that CO_2 molecule containing oxygen atom is different from N_2. And char + CO_2 may react in higher temperature zone. Therefore, in CO_2 atmosphere, when the temperature rises from 760 to 926°C, the mass loss rate of *C. vulgaris* is remarkably increased for the char gasification by CO_2 [34].

3.3. Effect of Heating Rates on Decomposition of C. vulgaris in N_2 Atmosphere. Figure 3 shows the DTG curve of *C. vulgaris* decomposition at the heating rates of 10, 20, and 40°C min^{-1} in N_2 atmosphere. The DTG curves for different heating rates (Figure 3) show that the rate of decomposition shifts to a higher magnitude as the heating rate increases, because the minimum heat required for the cracking of particles is reached later at higher temperatures, since the heat transfer is not as effective and efficient as slower heating rates [35]. As the heating rate increases from 10 to 20 and finally to 40°C/min, the maximum weight loss rate increases from 3.89 to 16.8%/min, and the corresponding temperature increases from 321.92 to 340.16°C, as shown in Table 3.

In addition, the initial degradation temperatures at different heating rates are slightly increased, while the final degradation temperature is decreased. So the temperature range of the main pyrolysis process is narrowed as the heating rate increased. Moreover, the similar findings are also found in the case of decomposition of rapeseed [36]. The average weight loss rate of whole temperature range (100–1000°C) is changed from 0.78 to 3.44%/min when the heating rate varies from 10 to 40°C/min (Table 3).

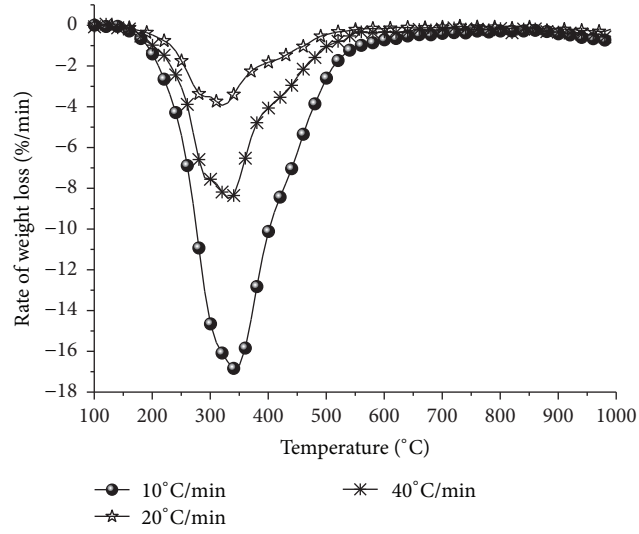

Figure 3: DTG curves of *Chlorella vulgaris* decomposition at the heating rates of 10, 20, and 40°C min^{-1} in N_2 atmosphere.

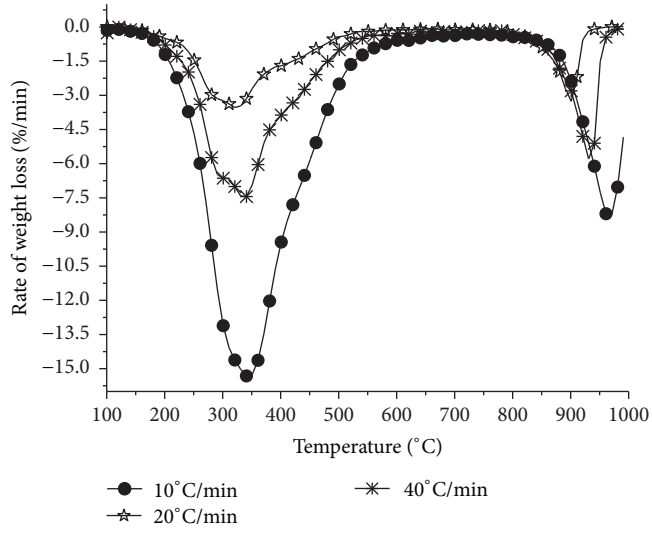

Figure 4: DTG curves of *Chlorella vulgaris* decomposition at the heating rates of 10, 20, and 40°C min^{-1} in CO_2 atmosphere.

3.4. Effect of Heating Rates on the Decomposition of C. vulgaris in CO_2 Atmosphere. The DTG curve of *C. vulgaris* decomposition at different heating rates in CO_2 atmosphere is shown in Figure 4. There are two peaks temperatures for each DTG curve: a strong peak (first peak) and one small one (second peak). As the heating rate increases, the two temperature peaks, especially the small one, shifts to high temperature.

Table 2: Results from thermogravimetric analysis for *Chlorella vulgaris* in different atmospheres with the heating rate of 10°C/min.

Atmosphere	Heating rate (°C/min)	T_1 (°C)	DTG_1 (% min^{-1})	T_2 (°C)	DTG_2 (% min^{-1})	DTG_{max} (% min^{-1})	Residual mass (%)
CO_2	10	323.8	−3.54	901.1	−3.26	−3.54	16.86
N_2	10	322	−3.94	—	—	−3.94	23.12

Note: T_1 is the temperatures for the first weight losses reaction peak; DTG_1 is the reaction rate for the first weight losses reaction peaks; T_2 is the temperatures for the second weight losses reaction peak; DTG_2 is the reaction rate for the second weight losses reaction peak; DTG_{max} is the maximum reaction rate.

Table 3: Results from thermogravimetric analysis in N_2 atmosphere with different heating rates.

Heating rate (°C/min)	T_I (°C)	T_{peak} (°C)	DTG_{peak} (%/min)	T_F (°C)	D_V (%/min)
10	165.35	321.92	−3.89	568.38	−0.78
20	171.37	330.01	−8.47	560.57	−1.67
40	176.73	340.16	−16.8	556.54	−3.44

Note: T_I, the initial degradation temperature; T_F, the final degradation temperature, T_{peak}, degradation peak temperature; DTG_{peak}, differential thermal gravity value at a peak temperature. D_V is the average weight loss rate of the temperature ranging from 100 to 1000°C.

When the temperature reaches to 531.15, 608.35, and 651.98°C, the first main decomposition process at the heating rates of 10, 20, and 40°C/min is completed. When the heating rate changes from 10 to 40°C/min, the maximum weight loss rates corresponding to the first peak temperature increase from 3.52 to 15.26, while the weight loss rate corresponding to the second peak temperature increase from 3.22 to 8.27°C/min. The average weight loss rate of whole temperature range (100–1000°C) is changed from 0.87%/min to 3.77%/min when the heating rate varies from 10 to 40°C/min (Table 4).

3.5. Kinetics Analysis. As shown in Figure 2, the *C. vulgaris* decomposition reaction in N_2 atmosphere is considered as a single pseudo component. But in CO_2 atmosphere, the decomposition process can be represented by the pseudo multicomponent overall model (PMOM) [31, 32, 37].

As mentioned in Section 3.1, in N_2 atmosphere, *C. vulgaris* mainly devolatilizes at 140–550°C, while in CO_2 atmosphere, the decomposition mainly occurs at 140–560°C and 790–1000°C (fourth stage), respectively.

The results on variance and correlation coefficient (R^2) are obtained from the experimental data analyzed with Excel 2003 software produced by Microsoft Corporation and Origin 7.0 software produced by Origin Lab Corporation.

Table 5 shows the kinetic parameters of *C. vulgaris* in N_2 and CO_2 atmosphere at a heating rate of 10°C min^{-1}. The correlation coefficient (R^2) between predicted and experimental values is 0.93684–0.99506 in two atmospheres, indicating that the predicted values can match the actual experimental values well (Table 5). The kinetic parameters of the second stage in N_2 atmosphere are E = 11.255 kJ/mol, n = 1.2, and A = 4.827, quite similar to those in CO_2 atmosphere (E = 9.863 kJ/mol, n = 1.1 and A = 2.361). This phenomenon is the same as that of the sewage sludge reported by Jindarom et al. [38]: in CO_2 atmosphere, the apparent activation energy and the reaction order of sewage sludge for low temperature are quite similar to those in N_2 atmosphere. However, the kinetic parameters of *C. vulgaris* in N_2 atmosphere are different from the reported *Chlorella protothecoides* (42.2~52.5 kJ·mol^{-1}) (Peng et al., 2001); it may be because the thermal behavior is greatly influenced by composition of biomass materials, and there may be obvious differences in decomposition kinetics among the similar species of biomass [13]. In addition, the values of kinetic parameters are varied depending on the assumptions decomposition kinetic models. Due to the different models used, the values may not be comparable [37].

As shown in Table 5, in CO_2 atmosphere, E = 9.863, 57.619, and 309.381 kJ/mol, n = 1.1, 1.6, and 7, and A = 2.361, 3757.358, and 6.520 × 1017 min^{-1} corresponding to the second, third and fourth stages of *C. vulgaris*. The maximum kinetic parameters (E, n, A) occur in the fourth stage, while the minimum values occur in the second one.

4. Conclusion

Thermogravimetric analysis is carried out to investigate decomposition characteristics of *C. vulgaris* in different atmospheres and different heating rates. It can be concluded as follows.

(1) In N_2 atmosphere, only one main decomposition stage occurs at 140–550°C (devolatilization). However, in CO_2 atmosphere, two main decomposition stages are observed, occurring at 140–560°C and 790–1000°C.

(2) At the heating rate of 10°C/min, there is only one peak for the DTG curve of *C. vulgaris* decomposition in N_2 atmosphere at 322°C and maximum rate of weight loss occurs at this peak. However, in CO_2 atmosphere, there are two peaks for the DTG curve of *C. vulgaris* decomposition at 323.8°C and 901.1°C, respectively, and the maximum rate of weight loss occurs at 323.8°C. Moreover, the total residual mass in CO_2 atmosphere (16.86%) is less than in N_2 atmosphere (23.12%).

(3) At the heating rate of 10°C/min, before 887°C, the weight loss in CO_2 atmosphere is less than that in N_2 atmosphere, while above 887°C, a new increase in the weight loss is observed in CO_2 atmosphere. In addition, when the temperature ranges 210–470°C, the mass loss rate of *C. vulgaris* decomposition in CO_2 atmosphere is lower than that in N_2 atmosphere, but it is opposite when the temperature is between 760°C and 926°C.

(4) As the heating rate increases, the maximum weight loss rate, temperature corresponding to the maximum weight

Table 4: Results from thermogravimetric analysis in CO_2 atmosphere with different heating rates.

Heating rate (°C/min)	T_I (°C)	T_1 (°C)	DTG_1 (°C/min)	T_2 (°C)	DTG_2 (°C/min)	T_F (°C)	D_V (%/min)
10	202.35	326.43	−3.52	900.79	−3.22	531.15	−0.87
20	233.54	336.21	−7.35	931.26	−5.7	608.35	−1.81
40	235.36	348.06	−15.26	969.82	−8.27	651.98	−3.77

Table 5: Kinetic parameters of *Chlorella vulgaris* at heating rate of 10°C min^{-1}.

stage	Gas	Model	E (kJ/mol)	n	A (min^{-1})	R^2
Second stage	N_2	PSOM	11.255	1.2	4.827	0.99321
	CO_2	PMOM	9.863	1.1	2.361	0.99506
Third stage	N_2	PSOM	—	—	—	—
	CO_2	PMOM	57.619	1.6	3757.358	0.93684
Fourth stage	N_2	PSOM	—	—	—	—
	CO_2	PMOM	309.381	7	6.520×10^{17}	0.97603

Note: R^2 is related coefficient.

loss rate, and the average weight loss rate in temperature range of 100–1000°C are increased.

(5) In CO_2 atmosphere, the maximum kinetic parameters (E, n, A) occur in the fourth stage, while the minimum kinetic parameters occur in the second one. The kinetic parameters of second stage in CO_2 atmosphere are quite similar to those in N_2 atmosphere.

Conflicts of Interest

The authors declare that they have no conflicts of interest regarding the publication of this paper.

Acknowledgments

This work was supported by the National Basic Research Program of China (973 Program): 2013CB228100; the National Natural Science Foundation of China (no. 50906025); General Administration of Quality supervision, Inspection of Public projects (no. 20140159); Guangdong Key Laboratory of Efficient and Clean Energy Utilization; and Key Laboratory of Efficient and Clean Energy Utilization of Guangdong Higher Education Institutes (KLB10004).

References

[1] S. S. Idris, N. A. Rahman, K. Ismail, A. B. Alias, Z. A. Rashid, and M. J. Aris, "Investigation on thermochemical behaviour of low rank Malaysian coal, oil palm biomass and their blends during pyrolysis via thermogravimetric analysis (TGA)," *Bioresource Technology*, vol. 101, no. 12, pp. 4584–4592, 2010.

[2] M. E. Alzate, R. Muñoz, F. Rogalla, F. Fdz-Polanco, and S. I. Pérez-Elvira, "Biochemical methane potential of microalgae biomass after lipid extraction," *Chemical Engineering Journal*, vol. 243, pp. 405–410, 2014.

[3] G. Guéhenneux, P. Baussand, M. Brothier, C. Poletiko, and G. Boissonnet, "Energy production from biomass pyrolysis: a new coefficient of pyrolytic valorisation," *Fuel*, vol. 84, no. 6, pp. 733–739, 2005.

[4] T. Wongsiriamnuay and N. Tippayawong, "Non-isothermal pyrolysis characteristics of giant sensitive plants using thermogravimetric analysis," *Bioresource Technology*, vol. 101, no. 14, pp. 5638–5644, 2010.

[5] X. G. Wang, Q. Liu, L. Tang, S. X. Guo, and C. Y. Liu, "Study on technique for reducing greenhouse gas CO_2," *Energy Environment Protection*, vol. 20, pp. 1–5, 2006 (Chinese).

[6] S. Grierson, V. Strezov, G. Ellem, R. Mcgregor, and J. Herbertson, "Thermal characterisation of microalgae under slow pyrolysis conditions," *Journal of Analytical and Applied Pyrolysis*, vol. 85, no. 1-2, pp. 118–123, 2009.

[7] J.-Y. Lee, C. Yoo, S.-Y. Jun, C.-Y. Ahn, and H.-M. Oh, "Comparison of several methods for effective lipid extraction from microalgae," *Bioresource Technology*, vol. 101, no. 1, pp. S75–S77, 2010.

[8] J. L. Ramos-Suárez and N. Carreras, "Use of microalgae residues for biogas production," *Chemical Engineering Journal*, vol. 242, pp. 86–95, 2014.

[9] C. Posten and G. Schaub, "Microalgae and terrestrial biomass as source for fuels—a process view," *Journal of Biotechnology*, vol. 142, no. 1, pp. 64–69, 2009.

[10] B. Sialve, N. Bernet, and O. Bernard, "Anaerobic digestion of microalgae as a necessary step to make microalgal biodiesel sustainable," *Biotechnology Advances*, vol. 27, no. 4, pp. 409–416, 2009.

[11] W. Peng, Q. Wu, P. Tu, and N. Zhao, "Pyrolytic characteristics of microalgae as renewable energy source determined by thermogravimetric analysis," *Bioresource Technology*, vol. 80, no. 1, pp. 1–7, 2001.

[12] D. Zhao, "Transient growth of flow disturbances in triggering a Rijke tube combustion instability," *Combustion and Flame*, vol. 159, no. 6, pp. 2126–2137, 2012.

[13] Z. Shuping, W. Yulong, Y. Mingde, L. Chun, and T. Junmao, "Pyrolysis characteristics and kinetics of the marine microalgae Dunaliella tertiolecta using thermogravimetric analyzer," *Bioresource Technology*, vol. 101, no. 1, pp. 359–365, 2010.

[14] M. M. Phukan, R. S. Chutia, B. K. Konwar, and R. Kataki, "Microalgae Chlorella as a potential bio-energy feedstock," *Applied Energy*, vol. 88, no. 10, pp. 3307–3312, 2011.

[15] A. Agrawal and S. Chakraborty, "A kinetic study of pyrolysis and combustion of microalgae Chlorella vulgaris using thermogravimetric analysis," *Bioresource Technology*, vol. 128, pp. 72–80, 2013.

[16] K. Kebelmann, A. Hornung, U. Karsten, and G. Griffiths, "Intermediate pyrolysis and product identification by TGA and Py-GC/MS of green microalgae and their extracted protein and lipid components," *Biomass and Bioenergy*, vol. 49, pp. 38–48, 2013.

[17] C. Chen, X. Ma, and K. Liu, "Thermogravimetric analysis of microalgae combustion under different oxygen supply concentrations," *Applied Energy*, vol. 88, no. 9, pp. 3189–3196, 2011.

[18] D. Zhao and J. Li, "Feedback control of combustion instabilities using a helmholtz resonator with an oscillating volume," *Combustion Science and Technology*, vol. 184, no. 5, pp. 694–716, 2012.

[19] D. Zhao, C. Ji, X. Li, and S. Li, "Mitigation of premixed flame-sustained thermoacoustic oscillations using an electrical heater," *International Journal of Heat and Mass Transfer*, vol. 86, pp. 309–318, 2015.

[20] D. López-González, M. Fernandez-Lopez, J. L. Valverde, and L. Sanchez-Silva, "Kinetic analysis and thermal characterization of the microalgae combustion process by thermal analysis coupled to mass spectrometry," *Applied Energy*, vol. 114, pp. 227–237, 2014.

[21] General Administration of Quality Supervision, Inspection and Quarantine of the People's Republic of China, and Standardization Administration of the People's Republic of China, *GB/T212-2008 Standard Test Methods for Coal Proximate Analysis*, Standards Press of China, 2009 (Chinese).

[22] Standardization Administration of the People's Republic of China, *GB211-84 Standard Test Methods for Coal Total Moisture*, Standards Press of China, 1985 (Chinese).

[23] American Society for Testing Materials International, "Standard test methods for instrumental determination of carbon, hydrogen, and nitrogen in laboratory samples of coal," ASTM D5373-08, ASTM International, 2008.

[24] American Society for Testing Materials International, "ASTM D5468-02 Standard Test Method for Gross Calorific and Ash Value of Waste Materials," 2007.

[25] American Society for Testing Materials International, "Standard test methods for analysis of wood fuels," ASTM E870-82(2006), American Society for Testing Materials International, 2006.

[26] H. Xiao and K. Liu, "Co-combustion kinetics of sewage sludge with coal and coal gangue under different atmospheres," *Energy Conversion and Management*, vol. 51, no. 10, pp. 1976–1980, 2010.

[27] Y. Zhaosheng, M. Xiaoqian, and L. Ao, "Thermogravimetric analysis of rice and wheat straw catalytic combustion in air- and oxygen-enriched atmospheres," *Energy Conversion and Management*, vol. 50, no. 3, pp. 561–566, 2009.

[28] A. A. Zuru, S. M. Dangoggo, U. A. Birnin-Yauri, and A. D. Tambuwal, "Adoption of thermogravimetric kinetic models for kinetic analysis of biogas production," *Renewable Energy*, vol. 29, no. 1, pp. 97–107, 2004.

[29] F. Carrasco, J. Gámez-Pérez, O. O. Santana, and M. L. Maspoch, "Processing of poly(lactic acid)/organomontmorillonite nanocomposites: microstructure, thermal stability and kinetics of the thermal decomposition," *Chemical Engineering Journal*, vol. 178, pp. 451–460, 2011.

[30] Z. Sun, J. Shen, B. Jin, and L. Wei, "Combustion characteristics of cotton stalk in FBC," *Biomass and Bioenergy*, vol. 34, no. 5, pp. 761–770, 2010.

[31] N. A. Liu, W. Fan, R. Dobashi, and L. Huang, "Kinetic modeling of thermal decomposition of natural cellulosic materials in air atmosphere," *Journal of Analytical and Applied Pyrolysis*, vol. 63, no. 2, pp. 303–325, 2002.

[32] J. J. M. Orfão, F. J. A. Antunes, and J. L. Figueiredo, "Pyrolysis kinetics of lignocellulosic materials—three independent reactions model," *Fuel*, vol. 78, no. 3, pp. 349–358, 1999.

[33] A. G. Barneto, J. A. Carmona, J. E. M. Alfonso, and L. J. Alcaide, "Use of autocatalytic kinetics to obtain composition of lignocellulosic materials," *Bioresource Technology*, vol. 100, no. 17, pp. 3963–3973, 2009.

[34] Q. Li, C. Zhao, X. Chen, W. Wu, and Y. Li, "Comparison of pulverized coal combustion in air and in O_2/CO_2 mixtures by thermo-gravimetric analysis," *Journal of Analytical and Applied Pyrolysis*, vol. 85, no. 1-2, pp. 521–528, 2009.

[35] T. Mani, P. Murugan, J. Abedi, and N. Mahinpey, "Pyrolysis of wheat straw in a thermogravimetric analyzer: effect of particle size and heating rate on devolatilization and estimation of global kinetics," *Chemical Engineering Research and Design*, vol. 88, no. 8, pp. 952–958, 2010.

[36] H. Haykiri-Acma, S. Yaman, and S. Kucukbayrak, "Effect of heating rate on the pyrolysis yields of rapeseed," *Renewable Energy*, vol. 31, no. 6, pp. 803–810, 2006.

[37] P. Thipkhunthod, V. Meeyoo, P. Rangsunvigit, B. Kitiyanan, K. Siemanond, and T. Rirksomboon, "Pyrolytic characteristics of sewage sludge," *Chemosphere*, vol. 64, no. 6, pp. 955–962, 2006.

[38] C. Jindarom, V. Meeyoo, T. Rirksomboon, and P. Rangsunvigit, "Thermochemical decomposition of sewage sludge in CO_2 and N_2 atmosphere," *Chemosphere*, vol. 67, no. 8, pp. 1477–1484, 2007.